NONTRADIONAL DETECTION OF SOIL MOISTURE CONTENT BASED ON HYPERSPECTRAL IMAGING TECHNIQUE

LONGGUO WU[*#], QIUFEI JIANG[1#], YAO ZHANG[2] AND SONGLEI WANG

School of Agriculture, Ningxia University, Yinchuan 750021, China

Keywords: Hyperspectral imaging technique, Soil, Moisture content, Non-destruction detection

Abstract

In the study, Vis-NIR hyperspectral imaging technique was investigated for non-destructive determination of soil moisture content. A total of 208 spectral information of soil samples by hyperspectral imaging system were collected. The differences between soil's moisture content and spectral changes were compared. Different methods of spectral data preprocessing methods, characteristic wavelengths extraction, and building models had influences on the performance of model established. Results from this investigation demonstrated that the reflectivity of soil spectrum were declining with the increase of soil moisture content. Once soil moisture content reached the limit of the field water holding capacity, the reflectivity of soil spectrum were increasing with the increase of soil moisture content. The methods of different pretreatment were analyzed, and the pretreatment method of normalization of unit vector was proposed. The number of characteristic wavelengths extracted by the method of uninformative variable eliminate (UVE), competitive adaptive reweighted sampling (CARS), beta coefficient (β), successive projections algorithm (SPA) were 49, 30, 5, 7, respectively. In order to reduce data redundancy, characteristic wavelengths extracted by the method of UVE and CARS were further extracted by SPA method. The number of characteristic wavelengths extracted by the method of UVE + SPA and CARS + SPA were 5, 8, respectively. The MLR model built based on the characteristic wavelengths extracted by the β coefficient was chosen as the best model, which of the optimal characteristic wavelengths were 411, 440, 622, 713, 790 nm, respectively. The correlation coefficient (Rp) and the root mean square error (RMSEP) for prediction set were 0.979 and 0.763, respectively. Therefore, it is feasible to predict soil moisture content using hyperspectral imaging technique.

Introduction

There are many water problems, such as shortage of water resources, the contradiction between supply and demand of water, which have become one of the important factors in restricting the sustainable development of economy in China. According to the statistics, a total of water resources every year in China was 2.8 trillion m^3 and ranked the sixth in the world (Qiu 2014). The contradiction in water supply and demand is particularly prominent and has been becoming a key factor of Ningxia Hui Autonomous Region's economic and social sustainable development and ecological environment evolution (Feng *et al.* 2006).

Soil moisture is an important parameter as the basic conditions of crop growth and development and forecasting model of crop's yield. The soil moisture not only has a direct influence on the growth of crops, but also some influences on the microclimate and soil mechanical properties (Liang *et al.* 2022). Soil moisture, as one of important natural components of soil, affects not only soil physical properties that contain bulk density, void and permeability, but also the nutrient dissolution and transportation and microbial activity of soil. The type of irrigation used here is not only a serious waste and low efficiency, but also easy to cause soil's secondary salinization (Zarabi and Jalali 2012). Therefore, it is of great practical significance for agricultural production to monitor surface soil moisture content, to determine the reasonable irrigation system, and reduce the occurrence of secondary salinization in soil.

---

[*] Author for correspondence: <wlg@nxu.edu.cn>. [#] These authors contributed to the work equally and should be regarded as co-first authors. [1]Animal Husbandry Extension Station, Yinchuan 750001, China. [2]Institute of Food Testing and Research, Yinchuan 750001, China.

Traditional monitoring soil moisture content methods are often invested through fixed-point of the field that has many shortcomings, such as time-consuming, strong soil destruction, less measurement points, and poor representation. At present, soil moisture content is measured by physical means that apply moisture molecules to quantify sample's characteristics, and mainly contain microwave monitoring (William *et al.* 2023, Bao *et al.* 2007, Qiao *et al.* 2006), thermal infrared monitoring (Wu *et al.* 2013), optical monitoring (Zhang and Li 2004, Yao *et al.* 2004). Due to different inversion moisture content methods in soil, the inversion effect is also very different.

A new spectral detection technology, named hyperspectral imaging technology, commonly used onboard or satellite borne imaging hyperspectral data sources(Galvao *et al.* 2008, Selige etal 2006, Gomez etal 2008). The partial least squares method was used to predict soil moisture content through Hyperion images, but results showed that the inversion accuracy of soil moisture content was very low (Zhang 2010). Hyperspectral imaging technology was used to invert the soil moisture content and adopt a variety of stoichiometric methods for analysis (Wei 2009). The relation between spectral reflectance and moisture content in soil surface was analyzed and achieved a good accuracy (Liu *et al.* 2004, Liu *et al.* 2011). The spectrum changes between moisture and salt in soil had a strong effect, and moisture content in soil was limited for different degrees of salinized soil (Liu *et al.* 2013). The studies above showed that the information extraction of soil moisture content based on hyperspectral imaging technology has practical feasibility, and achieves good results for relationship between different moisture content and spectrum of soil, which provide a method guidance and technical support for soil moisture monitoring. However, these methods are mostly as the research object of non-salted soil, and the effects of soil salinity on moisture and spectrum have not been considered to cause difficulty of application in arid areas.

The purpose of this study was to develop a hyperspectral imaging technique to predict soil moisture content. Because a hyperspectral image provides both spatial and spectral information, it is constructed in a three-dimensional data format with very high spectral redundancy. Thus, preprocessing methods and informative wavelengths selection are typically necessary to eliminate redundant variables and reduce noise in hyperspectral images. The specific objectives of this study were to (1) acquire the soil spectral responses using a region-based segmentation technique from hyperspectral images, (2) build a quantitative model between spectral data and measured moisture values of soil using chemometrics techniques, (3) obtain the informative wavelengths, (4) develop a prediction model of soil moisture content with the wavelengths selected, (5) evaluate the performance of the prediction model built through robustness and accuracy.

Material and Methods

The experiment of this study was conducted in 2016 in the surrounding area of Yinchuan City. The diversity of soil types is well suited for development of agricultural production and growth of various economic crops.

1. The 250 ml was taken in 11 beakers and was placed 100 g air dried soil in it. The soil salt content is less than 0.01% that means non-saline soil. Among 11 samples, one sample was treated as a control and the others samples were experiment groups and immediately sealed with a cling film. In order to ensure data accuracy, each soil sample was first carried out hyperspectral imaging and then weighed. The experiment lasted continuously 12 days.

2. Soil samples were collected with 3 cm diameter soil drilling in the experiment area, and each sample point that a total of four soil samples took depth of 0~10, 10~20, 20~30, and 30~40 cm soil was on the basis of S-line sampling. 100g soil was put into the sampling bag and number was sealed.

3. 30g weight of dry soil was filled with dry aluminum box and smoothed soil surface with a straight ruler. A gradient of 1, 2, 3, 4, 5, 6, 7, 8, 9, 10, 11, 12, 13, 14ml of moisture was injected, different gradient soil moisture content were obtained, such as 3, 6, 10, 13, 16, 20, 23, 26, 30, 33, 37, 40, 43, and 46%, respectively. The images of each sample were collected by hyperspectral imaging system and analyzed by Envi4.6 software.

4. A total of soil from undisturbed soil collected dry soil and loam in different sampling points and areas was 208 samples, which were used to attain images using hyperspectral imaging technology and measure the moisture content of soil by a halogen fast analyzer. The spectral features of soil images were extracted by Envi4.6 software to built the regression model using Unscrambler 10.4 software and Matlab R2014a software.

Soil samples were collected from depth 0-40 cm and kept in plastic bags in a manner to prevent soil moisture evaporation. The soil's moisture content is calculated using the weight moisture content formula (Wu 2017):

$$M(\%) = \frac{m_1 - m_2}{m_2} \times 100\% \qquad (1)$$

Where M is the moisture content of soil, m_1 is the original soil sample quality; m_2 is the mass of dried soil samples.

The CCD device in the hyperspectral imaging system attains noise and useful information on account of illumination distribution, different shapes, and existence of dark current. Hence, hyperspectral images obtained must be corrected. The original hyperspectral images (R_0) should be corrected based on black and white reference images, which will reduce the influence of illumination and the dark current of the camera. In this study, the acquired images were corrected using the following equation (Wu 2017):

$$R = \frac{R_o - D}{W - D} \times 100 \qquad (2)$$

Where R is the corrected hyperspectral image in a unit of relative reflectance (%), R_0 is the original hyperspectral image, D is the dark image for which there is almost no reflection, W is the white reference image that is almost total reflection.

The acquisition parameters of images include motor speed, exposure time, and object distance. For Vis-NIR hyperspectral imaging, the proper speed of the translation stage, exposure time, and object distance were set to 200 mm/s, 30 ms, 360 mm, respectively.

The samples were laid in a defined queue on the plate to be scanning by the hyperspectral imaging system. To conduct spectral data extraction from each subsample in the hyperspectral image, the region of interest (ROI) function of ENVI v4.6 software was used to isolate the subsample in different types of soil. The data analyses are conducted using the Unscrambler 10.4 software and Matlab R2014a software.

Results and Discussion

In order to obtain a certain gradient moisture content of each sample, eleven samples' initial soil moisture content were controlled 30%. The changes in moisture content and hyperspectral imaging spectra of samples on 1, 2, 3, 4, 5 and 12 days were measured and the results were shown in Figs 1 and 2.

It can be seen from Fig.1 that soil moisture content is gradually reduced along time increasing until the moisture content of the dried soil is reached at 0.3%. The decline rate of moisture content in the first day is larger than that of other days.

Along with time increasing, the changes between soil's moisture content and spectral exist a rule (Figs 1 and 2). The main reason is the evaporation free moisture of soil which enters directly the atmosphere from the soil surface from the first day to the second day. From the second day to the fifth day, the soil moisture mainly evaporates from the deep soil to the surface soil, and then into the atmosphere. Based on the theory of mass transferring, there is a gas film between the air and the surface soil, which existed a certain resistance that the process of mass transferring can't be ignored, as a result, the evaporation rate became slower and the average daily decreased by 2.6% per day. From the 5th day to the 12th day, soil's moisture content decreased from 17.7% to 0.3%.
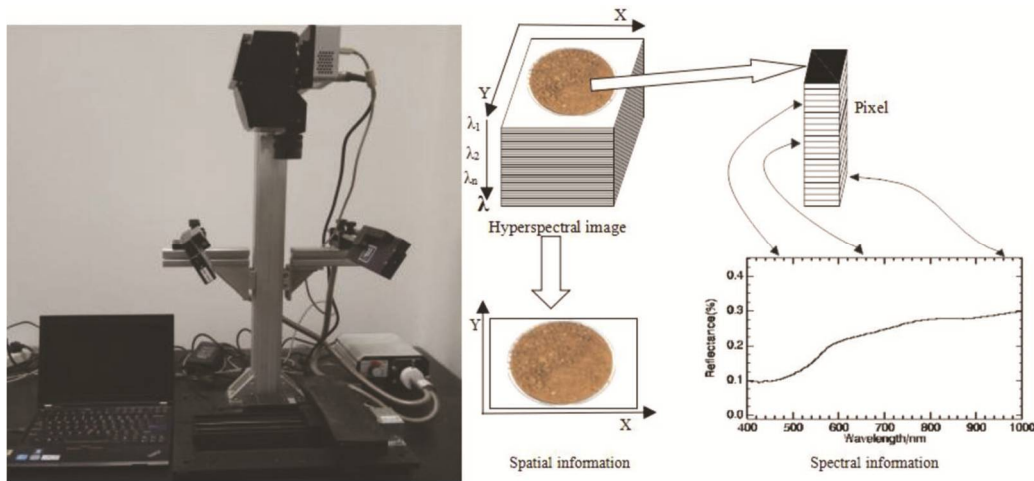
Fig. 1. Hyperspectral imaging system and data cube.
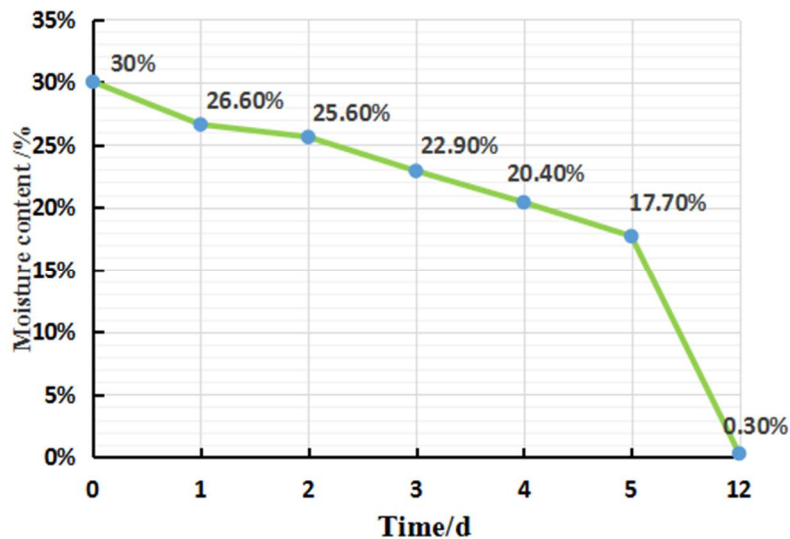
Fig. 2 Variation of soil moisture in different days.

In the experimental area, the spectral reflectance of different soil content in tree and field are shown in Fig. 3. It can be seen from Fig.3 that the decreases with the increase of the depth of the soil (10, 20, 30, 40 cm). The absorption between moisture molecules and the spectrum appeared a phenomenon that the less moisture molecules, less spectral absorption and the higher the reflectivity in the wavelength range of 400~1000 nm. It can be seen from Fig. 4 that the reflection spectra of dry soil and loam are different in different bands, which is also consistent with the conclusion (Wei 2009). The moisture content of the soil in the 10-30 cm soil followed the law of
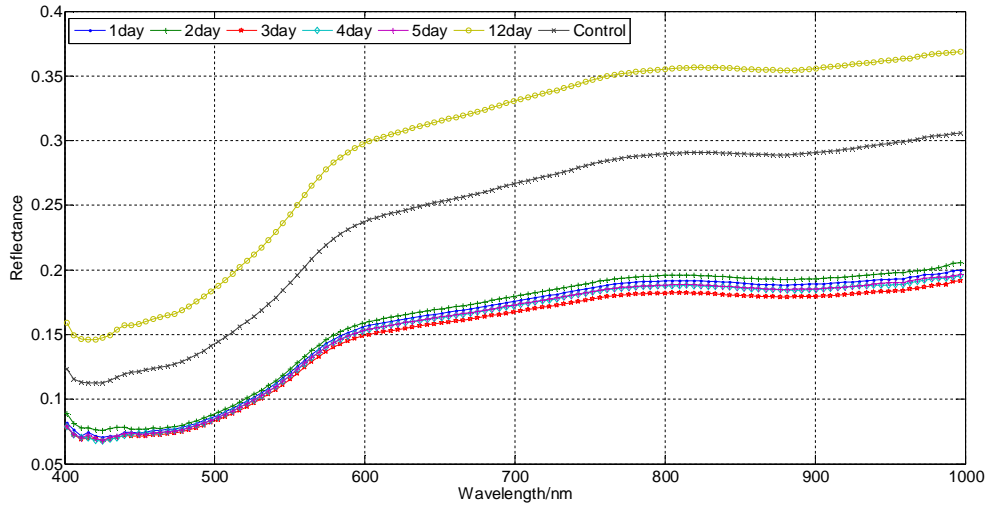
Fig. 3. Soil spectrum curves for different days (400-1000 nm).
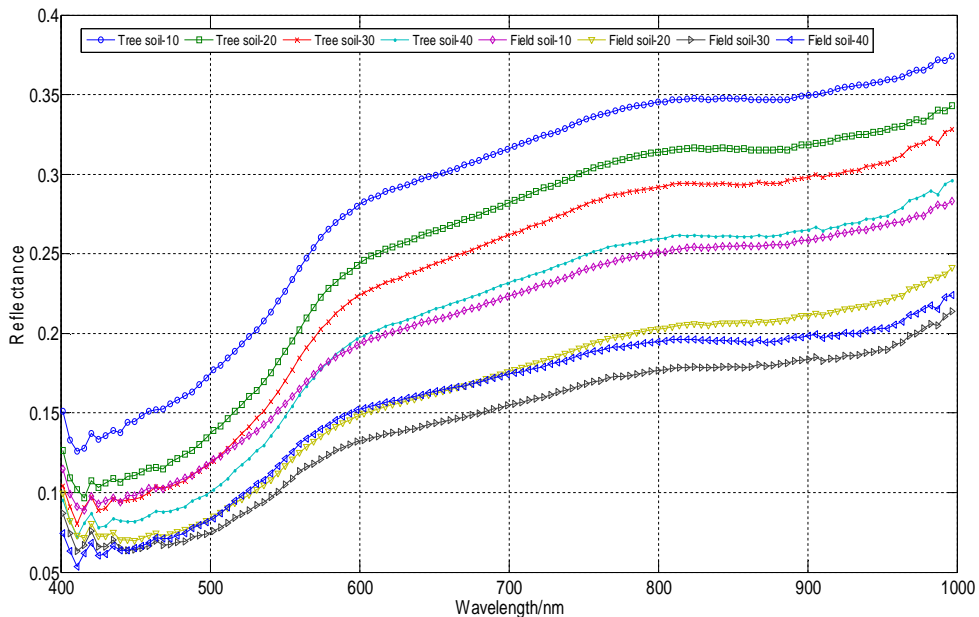
Fig. 4. Hyperspectral curves of soils at different depths (400-1000 nm).

 "soil's moisture content increases along with the reflectivity decreases" (Figs 3 and 4), which was consistent with the results of Wei Na (2009). While the reflectance of the soil in the 40 cm field increased, mainly due to the moisture content of the soil in the 40 cm field exceeding moisture capacity of the field, soil surface will appear a moisture film, hindering the absorption of moisture molecules in the soil, increasing the spectral reflectance value, resulting spectral reflectance value increases along with the increase of moisture content of soil. This also provides the basis for the qualitative diagnosis of soil's moisture content in the future.

From the Fig. 5, the original spectral curve existed a serious baseline drift phenomenon in the wavelength range of 400~1000nm. As there is the phenomenon of baseline drift, so it is essential to take a pretreatment for the original spectral data.
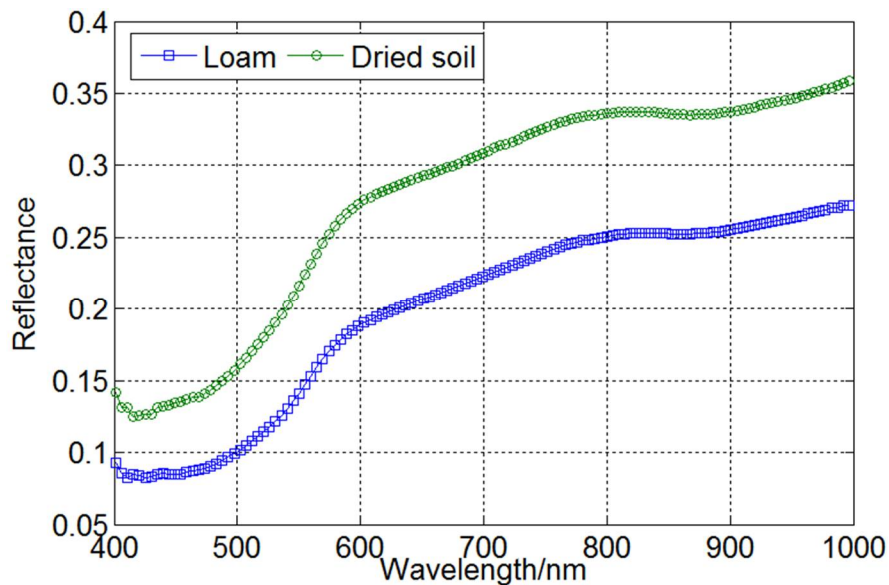
Fig. 5. Average spectra of dry soil and loamy soil (400-1000 nm).

It can be seen from Table 1 that the maximum and minimum values of the prediction set are within the range of the calibration set, and both of the average value is 5.98% and the variance of calibration set is almost as same as predication set.

It can be seen from Table 2 that the PLSR model of original spectra differed significantly from PLSR models of different pretreatment spectra. Comparison of the models of original spectrum and 24 types of pretreatment spectra, the area normalization and mean normalization method were optimized and has same effect. Therefore, area normalized pre-treatment spectrum was chosen in the wavelength range of 400~1000nm.

In order to reduce the data processing capacity, the feature wavelengths were extracted from the area normalized spectrum in 400~1000nm. Different extraction important wavelengths manners were employed, such as β coefficient, uninformative variable eliminate (UVE), successive projections algorithm (SPA), competitive adaptive reweighted sampling (CARS) in Fig.6. Table 3 shows the results of the comparison of different characteristic wavelength extraction methods.

Table 1. Determination of soil moisture content.

Sample set	NO.	Maximum value (%)	Minimum value (%)	Average value (%)	Variance (%)
Calibration set	156	11.21	1.15	5.98	3.59
Validation set	52	10.77	1.43	5.98	3.6

Table 2. PLSR model of different pretreatment spectral (400-1000 nm).

Types	PCs	R_C	RMSEC	R_{CV}	RMSECV	R_P	RMSEP
Original spectrum	3	0.951	1.109	0.947	1.15	0.944	1.186
3 points of smoothing	2	0.946	1.16	0.944	1.187	0.947	1.147
5 points of smoothing	2	0.946	1.161	0.943	1.187	0.947	1.145
7 points of smoothing	2	0.946	1.161	0.943	1.188	0.947	1.143
9 points of smoothing	2	0.946	1.161	0.943	1.188	0.947	1.143
3 point of Gaussian filtering	6	0.972	0.842	0.968	0.903	0.96	1.053
5 point of Gaussian filtering	3	0.95	1.113	0.947	1.153	0.943	1.187
7 point of Gaussian filtering	3	0.95	1.115	0.947	1.155	0.943	1.186
3 point of median filter	3	0.951	1.112	0.947	1.152	0.943	1.188
5 point of median filter	3	0.95	1.12	0.946	1.16	0.943	1.189
7 point of median filter	3	0.949	1.124	0.946	1.165	0.943	1.186
3 point of 3 convolution of smoothing	3	0.951	1.11	0.947	1.151	0.944	1.187
5 point of 3 convolution of smoothing	3	0.951	1.111	0.947	1.152	0.944	1.187
Area normalization	**5**	**0.984**	**0.637**	**0.982**	**0.672**	**0.979**	**0.764**
Unit vector normalization	1	0.965	0.943	0.964	0.955	0.965	0.965
Average normalization	5	0.984	0.637	0.982	0.672	0.979	0.764
Maximum normalization	2	0.963	0.964	0.962	0.985	0.96	1.027
Threshold normalization	2	0.959	1.016	0.957	1.042	0.953	1.095
First order derivative 3 point convolution	4	0.967	0.917	0.957	1.039	0.137	4.322
First order derivative 1 point convolution	4	0.97	0.872	0.958	1.03	0.356	4.761
Second derivative 3 point convolution	7	0.931	1.31	0.891	1.628	-0.763	15.84
Second order derivative 1 point convolution	5	0.95	1.117	0.912	1.472	-0.837	14.32
SNV	6	0.98	0.705	0.972	0.84	0.979	0.808
MSC	6	0.978	0.749	0.969	0.886	0.977	0.839
OSC	3	0.969	0.882	0.965	0.945	0.955	7.708

From Table 3, as the UVE and CARS methods extracted more characteristic wavelengths, the SPA method is used to further extraction feature wavelengths in order to reduce the data redundancy in the400~1000nm. The number of characteristic wavelengths extracted by UVE reduced from 49 to 5, and the number of characteristic wavelengths extracted by CARS reduced from 30 to 8. The number of the characteristic wavelengths by PLSR and SPA methods extracted was 5 and 7.
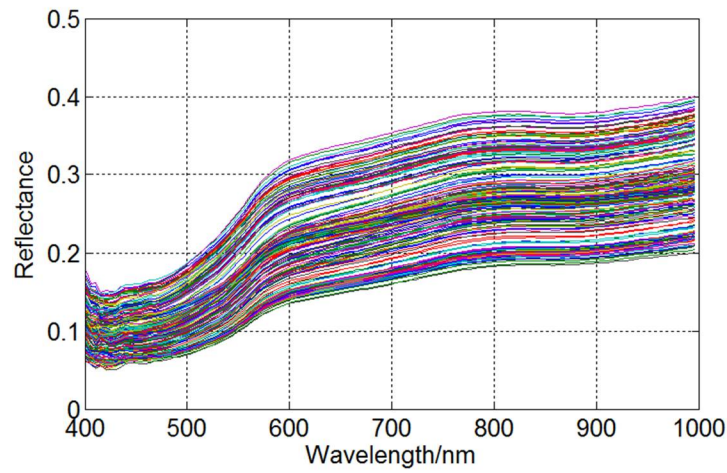
Fig. 6. Spectral curves of all samples of dry soil and loam.
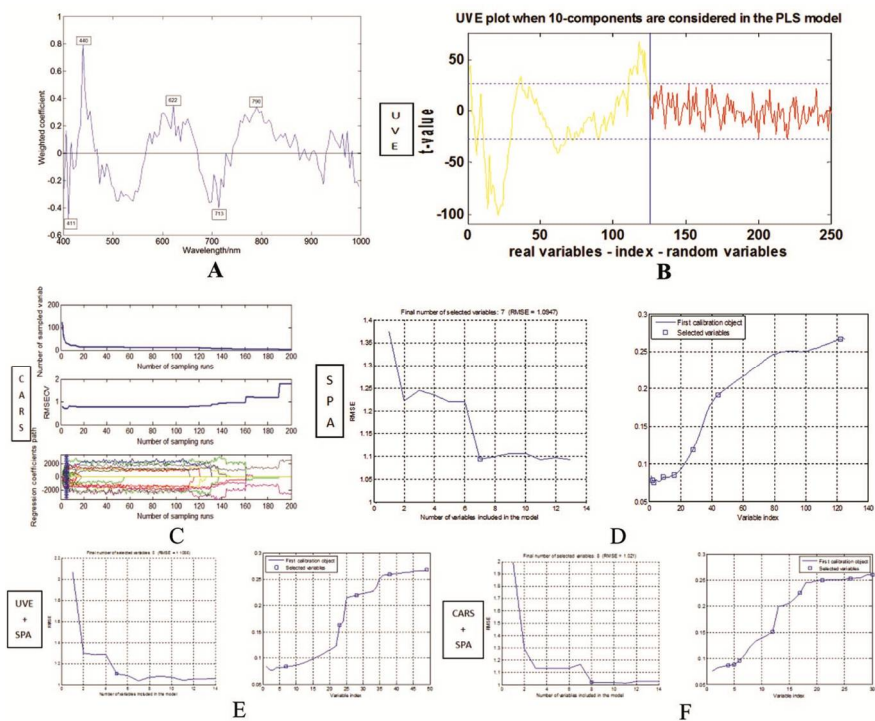
Fig. 7. Different characteristic wavelength extraction method (400-1000 nm).

In order to optimize the models of the characteristic wavelength, MLR, PCR and PLSR methods were used to compare the different characteristic wavelengths extracted. The results were shown in Table 4. From Table 4, compared with the MLR, PCR, PLSR model, the MLR model of the same type of characteristic wavelength of extraction manners is superior to the others models established.

Table 3. Comparison of different characteristic wavelength extraction methods.

Wavelength/nm	Feature wavelength extraction method	NO.	The band or wave number of Extraction
400-1000	β coefficient	5	411, 440, 622, 713, 790
	UVE	49	1, 2, 6, 11, 12, 13, 14, 15, 16, 17, 18, 19, 20, 21, 22, 23, 24, 25, 26, 27, 28, 29, 36, 37, 59, 60, 61, 62, 63, 64, 65, 66, 67, 72, 90, 111, 112, 113, 114, 115, 116, 117, 118, 119, 120, 121, 122, 123, 124
	CARS	30	9, 17, 21, 23, 24, 27, 31, 35, 37, 38, 39, 40, 55, 56, 59, 65, 72, 85, 86, 90, 93, 94, 97, 100, 109, 110, 112, 114, 120, 121
	SPA	7	2, 3, 9, 16, 28, 44, 122
	UVE+SPA	5	7, 23, 28, 38, 49
	CARS+SPA	8	4, 5, 6, 12, 17, 21, 26, 30

Table 4. Comparison of different model of extracted characteristic wavelengths (400-1000 nm).

Method	Type	PCs	R_C	RMSEC	R_{CV}	RMSECV	R_P	RMSEP
MLR	β coefficient	—	0.981	0.706	0.979	0.728	0.979	0.763
	UVE	—	0.992	0.542	0.98	0.721	0.98	0.711
	CARS	—	0.992	0.492	0.988	0.562	0.97	0.878
	SPA	—	0.977	0.789	0.974	0.82	0.971	0.875
	UVE+SPA	—	0.973	0.847	0.97	0.871	0.963	0.972
	CARS+SPA	—	0.971	0.889	0.967	0.92	0.969	0.892
PCR	β coefficient	2	0.966	0.926	0.965	0.946	0.965	0.959
	UVE	2	0.968	0.9	0.967	0.919	0.962	0.993
	CARS	1	0.964	0.923	0.963	0.963	0.965	0.942
	SPA	2	0.965	0.933	0.964	0.955	0.963	0.972
	UVE+SPA	1	0.965	0.936	0.964	0.947	0.966	0.927
	CARS+SPA	3	0.97	0.875	0.968	0.901	0.968	0.894
PLSR	β coefficient	5	0.981	0.692	0.979	0.726	0.979	0.763
	raw	5	0.984	0.637	0.982	0.672	0.979	0.764
	UVE	2	0.968	0.896	0.967	0.916	0.963	0.989
	CARS	1	0.965	0.945	0.964	0.957	0.966	0.941
	SPA	3	0.973	0.824	0.97	0.866	0.972	0.846
	UVE+SPA	1	0.965	0.934	0.965	0.946	0.966	0.926
	CARS+SPA	3	0.97	0.873	0.968	0.903	0.968	0.891

In summary, the MLR model of the characteristic wavelength of the β coefficient extraction is preferred in the 400-1000 nm. The predicted correlation coefficient is 0.979 and the RMSE of the mean square error is 0.763.

In this paper, soil moisture content was measured by Vis-NIR hyperspectral spectroscopy (spectral range400~1000nm). The soil's moisture content and spectral variation were measured and compared along with different days. The results show that the reflectivity of the spectral curve decreases with the increase of soil moisture content, and the reflectivity of the spectral curve increases with the increase of soil's moisture content when it increases beyond the field moisture holding capacity.

The method of different pretreatment is analyzed and the optimal pretreatment method that is area normalization was obtained. The characteristic wavelengths are extracted by different manners in the wavelength range of 400~1000nm, and the number of characteristic wavelengths extracted by the UVE, CARS, β coefficient and SPA methods is 49, 30, 5 and 7, respectively. In order to reduce the data redundancy, feature wavelengths extracted by UVE and CARS manners were further extracted by SPA manners. The number of characteristic wavelengths extracted by UVE + SPA and CARS + SPA was 5 and 8, respectively. On the basis of this, the MLR, PCR and PLSR methods were used to establish the model based on the characteristic wavelengths extracted in 400~1000nm. The MLR model of the characteristic wavelengths extracted by *β* coefficient was chosen. The optimal characteristic wavelengths are 411, 440, 622, 713, 790 nm, respectively. The correlation coefficient predicted of optimal model was 0.979 and the RMSEP is 0.763. Therefore, soil moisture content can be quantitatively analyzed in different bands in future.

References

Bao YS, Liu LY and Wang JH 2007. Soil moisture estimation based on optical and microwave remote sensing data, Journal of Beijing Normal University (Natural Science) **43**(3): 228-233.

Feng SY, Chen SJ, Huo ZL and Li WC 2006. Review on the present situation and future prospect of moisture resource carrying capacity in China, Journal of East China University of Technology (Natural Science), **29**(4): 301-306.

Galvao LS, Formaggio AR, Couto EG and Roberts DC 2008. Relationships between the mineralogical and chemical composition of tropical soils and topography from hyperspectral remote sensing data, ISPRS Journal of Photogrammetry and Remote Sensing **63**(2): 259-271.

Gomez C, Rossel RV and McBratney AB 2008. Soil organic carbon prediction by hyperspectral remote sensing and field VIS- NIR spectroscopy: An Australian case study, Geoderma, **146**(4): 403-411.

Liang XY, Xin ZB, Shen HY and Yan TF 2022. Deep soil water deficit causes Populus simonii Carr degradation in the three north shelterbelt region of China, Journal of Hydrology, 612, pp, 1-13.

Liu Y, Pan XZ, Wang CK, Li YL, Shi RJ, Zhou R and Xie XL 2013. Predicting soil salinity based on spectral symmetry under wet soil condition, Spectroscopy and Spectral Analysis **10**: 2771- 2776.

Liu WD, Baret F, Zhang B, Zhen LF and Tong QX 2004. Extraction of soil moisture information by hyperspectral remote sensing, Acta Pedologica Sinica **41**(5): 700-706.

Liu H, Sun JS and WCC 2011. Research status and development trend of the effect of irrigation on vegetable quality, China Rural Water Resources and Hydropower, 36, 04, pp.81-84.

Qiao PL, Zhang JX and Wang CH 2006. Soil moisture retrieving by passive microwave remote sensing data, Journal of Liaoning Technical University (Natural Science), 25, 3, pp.342-344.

Qiu RJ 2014. Moisture and heat dynamics and simulation in soil-plant system in greenhouse. China Agricultural. University.

Selige T, Bhner J and Schmidhalter U 2006. High resolution topsoil mapping using hyperspectral image and field data in multivariate regression modeling procedures, Geoderma, 136, 1/2, pp.235-244.

Wei N 2009. The study of applying hyper-spectral remote sensing technology in soil moisture monitoring. Chinese Academy Agricultural Sciences.

William GS, Evan LH, Jerome A, Soumen M and Oliver AW 2023. *In situ* monitoring of microwave plasma-enhanced chemical vapour deposition diamond growth on silicon using spectroscopic ellipsometry, 202, 1, pp.204-212.

Wu LG 2017. Research on Diagnosis Mechanism and Model of Soil's Water and Salt Content and Tomato Plants' Moisture Based on Hyperspectral Imaging Technique, Ningxia University.

Wu J, Liu MS and Li WT 2013. Inversion technology of soil's moisture content based on hyperspectral imaging unmixing, Bulletin of Soil and Water Conservation 5: 156-160.

Yao CS, Zhang ZX and Wang X 2004. Evaluating soil moisture status in Xin Jiang using the temperature vegetation dryness index (TVDI), National Remote Sensing Bulletin **19**(6): 473-478.

Zarabi M and Jalali M 2012. Leaching of nitrogen from calcareous soils in western Iran: a soil leaching column study, Environmental Monitoring & Assessment, 184, 12, pp.7607-7622.

Zhang CG and Li W 2004. Study on Remote Sensing Monitoring Application of Drought Disaster in Fujian Province, Meteorological. **30**(3): 22-24.

Zhang TT 2010. Partial Least Squares Modeling of Hyperspectral Remote Sensing for Mapping Agricultural Soil Properties. Jilin University.